HIGH TEMPERATURE OXIDATION AND EROSION-OXIDATION BEHAVIOR OF STEELS[1]

S.M.C.Fernandes[2]
O. V. Correa[3]
L. V. Ramanathan[4]

Abstract
The high temperature oxidation and erosion-oxidation (E-O) behavior of steels AISI 1020, 304, 310 and 410 were determined. The oxidation behavior was determined in a thermogravimetric analyzer and a test rig in which a specimen assembly was rotated through a fluidized bed of alumina particles (200μm) was used to determine the E-O behavior. The E-O tests were carried out in the range 25 - 600ºC, with average particle impact velocities of 6, 14 and 30 ms^{-1} at an impact angle of 90º. The oxidation tests revealed mainly parabolic behavior and the surface oxides to be a mix of Fe_2O_3, Fe_3O_4, FeO and Cr_2O_3, depending on steel composition. In the E-O tests, wastage varied with temperature and particle impact velocity. Depending on the impact velocity, a transition in the dominant wastage mechanism occurred and the transition temperature varied with steel composition. E-O maps of the steels indicating low, moderate and severe wastage zones were prepared to aid in materials selection for industrial applications.
Key words: Oxidation; Erosion-oxidation; Wastage; Steels.

COMPORTAMENTO DE OXIDAÇÃO E EROSÃO-OXIDAÇÃO DE AÇOS EM TEMPERATURAS ELEVADAS

Resumo
Neste estudo foram determinados os comportamentos de oxidação e erosão-oxidação (E-O) de aços AISI 1020, 410, 304 e 310 em temperaturas elevadas. O comportamento de oxidação foi avaliado em analisador termogravimétrico. Foi utilizado um aparato no qual um arranjo de corpos de prova dos aços giraram por um leito fluidizado de partículas de alumina (200μm) para avaliar o comportamento de E-O. Foram conduzidos os ensaios de E-O na faixa de temperatura 25 – 600° C, as velocidades médias de impacto das partículas de 6, 14 e 30 ms^{-1}, e ao ângulo de impacto de 90°. Os ensaios de oxidação mostraram comportamento parabólico principalmente, e os óxidos nas superfícies sendo uma mistura de Fe_2O_3, Fe_3O_4, FeO e Cr_2O_3, dependendo da composição do aço. Nos ensaios de E-O, o desgaste variou com temperatura e velocidade de impacto das partículas. Dependendo da velocidade de impacto, ocorreu uma transição no mecanismo dominante de desgaste e a temperatura da transição variou com a composição do aço. Foram preparados mapas de E-O indicando zonas de desgaste baixo, moderado e severa para auxiliar na seleção dos aços.
Palavras chaves: Oxidação; Erosão-oxidação; Desgaste; Aços.

[1] *Technical contribution to 63rd ABM Annual Congress, July, 28th to August 1st, 2008, Curitiba – PR – Brazil.*
[2] *Dra. IPEN, Av. Prof. Lineu Prestes 2242, São Paulo, Brasil.*
[3] *Técnico, IPEN, Av. Prof. Lineu Prestes 2242, São Paulo, Brasil.*
[4] *Ph.D, Gerente do CCTM, IPEN, Av. Prof. Lineu Prestes 2242, São Paulo, Brasil.*

1 INTRODUCTION

The room temperature erosion behavior of metallic and ceramic materials has been extensively studied.[1-3] Nevertheless, correlations between erosion properties and physical parameters of many materials still remain vague. The high temperature oxidation behavior of various metals and alloys is well documented but only limited information is available about the conjoint effect of erosion and oxidation at high temperatures. The results of some erosion-oxidation (E-O) studies have shown synergy between erosion and oxidation, indicating that degradation caused by E-O can be greater than the sum of degradation caused by erosion and oxidation processes operating separately.[4-6] There are also references to surface oxide scales inhibiting erosion.[7] That is, the wastage rate under E-O conditions being lower than that in the absence of oxidation. These contrary observations have generated, in recent years, increased attention about E-O processes.

E-O interactions have been described in terms of regimes.[4] Kang et al.[8] proposed the existence of four regimes as a function of increasing temperature, based on E-O studies of pure metals. These regimes were termed: (a) erosion of metal, which predominated at low temperatures; (b) oxidation affected erosion, where the oxide and the metal eroded; (c) erosion-enhanced oxidation, during which more oxide formed as it was eroded and (d) oxide erosion, where only the oxide eroded. Modifications to these regimes and other interpretations about the existence of a variety of other sub E-O regimes have been proposed. [9,10] Definition of E-O regimes has varied significantly, both in the number of regimes that have been proposed as well as in the criteria for defining transitions.[11] Justifications for the various regimes depended on the E-O conditions and experimental evidence put forth to support the transitions. This signifies that there is potentially a number of interaction regimes depending on the criteria used to define the transitions.

Adequate procedures to select materials to resist E-O degradation at high temperatures are presently not available. Presently, a variety of metallic and ceramic materials, composites and cermets are used in industrial applications where E-O conditions prevail. The metallic materials include a variety of alloys meant for medium and high temperature applications. The criteria often used in many industries to select alloys for components subject to E-O conditions are hardness, cost and availability.

To provide further input to aid material selection for high temperature applications where E-O conditions prevail, studies were carried out to evaluate the E-O behavior of some commonly used steels. This paper presents the high temperature oxidation and E-O behavior of AISI 1020, 304, 310 and 410. The E-O measurements were made in a test rig in the temperature range 25°C - 600°C, using alumina particles as the erodent at average impact velocities of up to 30 ms^{-1}.

2 METHODS AND MATERIALS

The chemical composition of the steels AISI 1020, 304, 310 and 410, used in this investigation is shown in Table 1. Specimens for the oxidation and E-O tests were cut to size from ‘as-received’ steel sheets, cleaned and degreased ultrasonically in acetone.

Isothermal oxidation measurements were carried out in a thermogravimetric analyzer at temperatures that ranged from 100 to 1000°C and weight gain versus time plots were obtained.

A schematic diagram of the E-O test rig is shown in Figure. 1. In this rig a specimen assembly was rotated through a fluidized bed of erodent particles. Alumina powder in the size range 212-150 μm was used as the erodent. The fluidized bed of particles was obtained by pumping pre-heated air through a porous plate supporting a bed of erodent particles. Fluidization of the erodent particles was done within a furnace and the particle impact velocity (PIV) on the test specimens was controlled by a motor that rotated the specimen assembly.

Table 1. Steel composition determined by x-ray fluorescence spectroscopy.

Steel	Elements (weight %)								
AISI	C	Cr	Ni	Mo	Mn	Si	P	Cu	Fe
1020	0.15	-	-	-	0.33	-	-	-	Balance
304	0.07	18.7	8.0	0.03	1.4	0.6	0.04	0.09	Balance
310	0.07	24.1	19.1	0.07	1.7	0.5	-	0.1	Balance
410	0.04	11.5	0.18	-	0.14	0.5	0.4	-	Balance

The E-O test specimens were weighed and fixed with AISI 310 screws to the specimen holder in the E-O test rig. The specimens were positioned at the end of a crossed specimen holder. The E-O test conditions were: (a) temperatures - R.T., 100, 200, 300, 400, 500 and 600°C; (b) erodent impact angle of 90° at average PIV of 6 (V1), 14 (V2) and 30 (V3) ms^{-1}. After the tests, the specimens were weighed, examined in a scanning electron microscope and their surface reaction products analyzed by EDS.

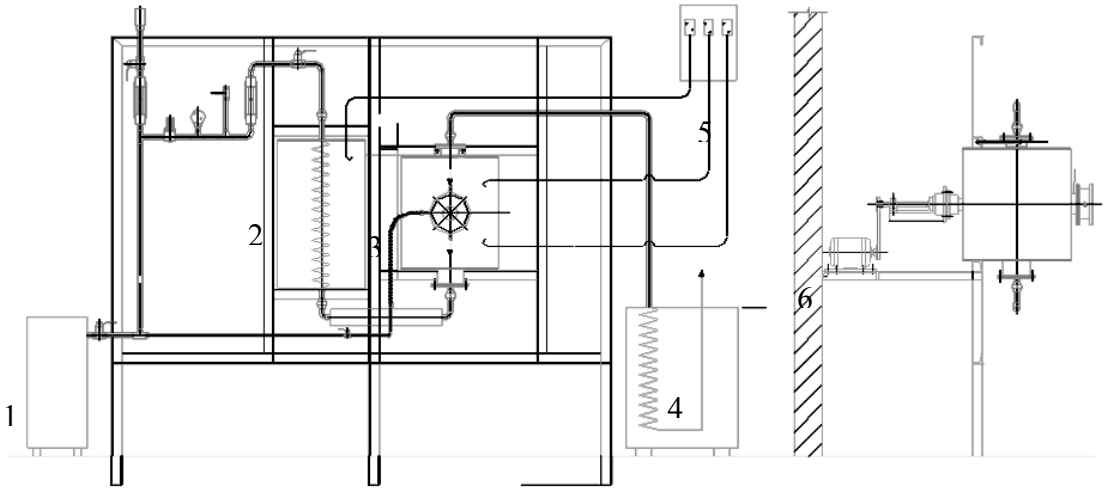

Figure 1. Schematic diagram of the E-O test rig: 1- compressor; 2- pre-heating furnace; 3- E-O furnace; 4- system for particle retention and cooling; 5- control panel; 6- motor to rotate the specimens through particle bed in the furnace.

3 RESULTS AND DISCUSSION

3.1 Oxidation Behavior of the Steels

Isothermal oxidation curves at the different temperatures in the range 100-1000° C were determined. The oxidation behavior of all the steels, except AISI 1020 was mainly parabolic. AISI 1020 showed higher oxidation rates at all the temperatures due to the formation of Fe_2O_3 and Fe_3O_4 up to 570° C and non-protective FeO above this temperatures. The oxides formed on the other steel surfaces were: (a) AISI 410 - Fe_2O_3 and $(Fe, Cr)_2O_3$; (b) AISI 304 - Fe_2O_3, Fe_3O_4, Cr_2O_3; (c) AISI 310 - Cr_2O_3.

3.2 Erosion-oxidation Behavior of the Steels

Figure 2 shows the wastage or weight loss of the steels as a function of E-O test temperature at PIVs of V1, V2 and V3. Figure 2a shows that at V1, the wastage of the steels did not vary much up to 300° C. Above this temperature and up to 400° C all the steels except AISI 304 revealed an increase in wastage due to removal of both the surface oxide and the substrate by particle erosion. This increase in wastage is followed by a decrease at higher temperatures, indicating higher weight gain due to oxide formation compared to weight loss by particle erosion. This transition takes place at 400° C for AISI 310, at 450° C for AISI 1020, at 480° C for AISI 410 and at 510° C for AISI 304. At V2, shown in figure 2b, the overall wastage was very low. All the steels revealed slight increases in weight up to 200° C and a behavior quite similar to that observed at V1. The Y-axis of this figure is expanded and should be borne in mind during comparisons. Slight wastage can be observed in the temperature range 200-300° C. This can be attributed to two conjoint processes taking place. Weight loss due to erosion and weight gain due to embedded erosive particles.

In the range 200-500° C, the slight variations in wastage of the steels are due to a combination of effects: oxide erosion, new oxide formation and embedded particles. Above this temperature range, wastage decreases, and this marks the transition from the oxidation-aided-erosion-regime to the oxidation-controlled-regime.

Figure 2c shows the wastage behavior at V3. Marked wastage is observed at temperatures up to 100° C. This is due mainly to erosion of the surface oxide and the substrate. Above this temperature, the wastage decreases due to the combined effects of new oxide formation and embedded particles. The wastage of AISI 1020 and AISI 410, both Fe_3O_4 and/or Fe_2O_3 formers, increases above 300° C, decreases after 400° C and again increases beyond 500° C. The wastage of the other steels, AISI 304 and AISI 310, both chromium dioxide formers, remained almost constant up to 500° C. All the steels revealed increased wastage above 500° C. This transition, observed at 500° C and V3 is the same as that observed at 300° or 400° C and V1. This wastage increase, at higher temperatures with increase in PIV has been reported in other papers.[11] The shift to lower wastage, observed at 400° C or 500° C at V1 probably occurs at temperatures above 600° C at V3. The reduction in wastage at these temperatures is due to a transition from oxidation-aided-erosion-regime to oxidation-controlled-regime. Similar observations have been reported.[11]

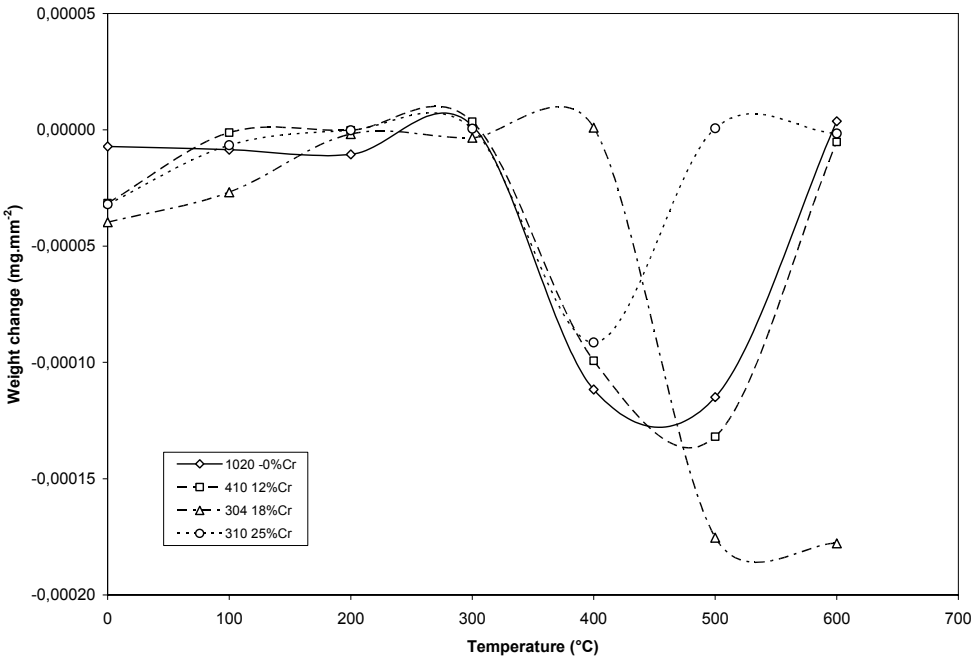
0,00005
0,00000
-0,00005
-0,00010
-0,00015
-0,00020
Weight change (mg.mm-2)
0
100
200
300
400
500
600
700
Temperature (°C)
1020 -0%Cr
410 12%Cr
304 18%Cr
310 25%Cr

(a)

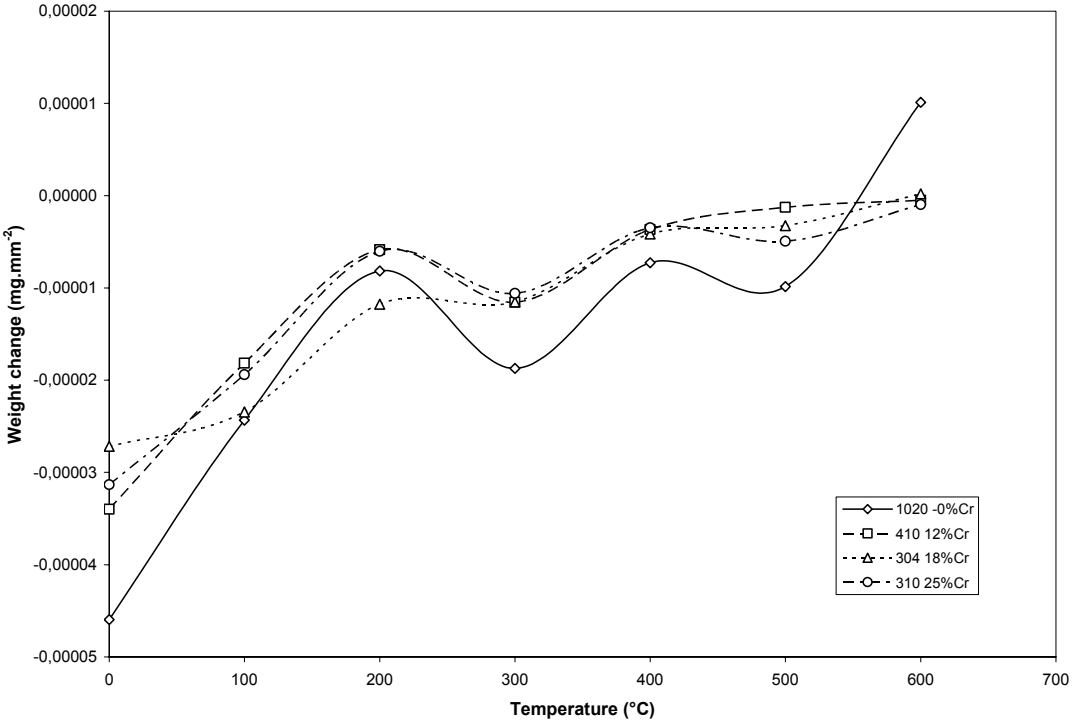
0,00002
0,00001
0,00000
-0,00001
-0,00002
-0,00003
-0,00004
-0,00005
Weight change (mg.mm-2)
0
100
200
300
400
500
600
700
Temperature (°C)
1020 -0%Cr
410 12%Cr
304 18%Cr
310 25%Cr

(b)

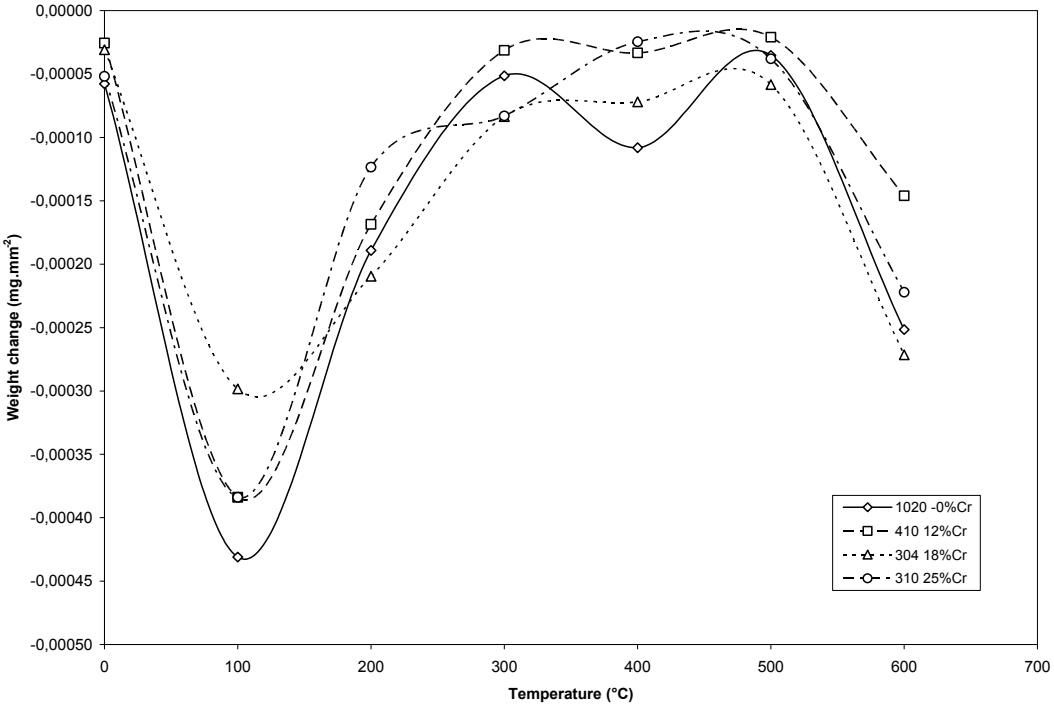

(c)

Figure 2. Wastage of the steels (in mg/mm^2) as a function of E-C test temperature and with particle impact velocities: (a) V1; (b) V2 and (c) V3.

The oxide formed on AISI 1020 is a mixture of Fe_2O_3 and Fe_3O_4 at the lower temperatures and FeO at the higher temperatures. Fe_2O_3 is more ductile and with higher resilience to particle impact. On the other hand, FeO is brittle and easily removed upon particle impact. On the other Cr containing steels, the oxide formed is a mixture of Fe and Cr oxides, depending on the Cr content of the steel. In the initial stages iron oxide forms and later the layers close to the metal-oxide interface consist of Cr_2O_3. The external iron oxide layer is easily removed by particle impact leaving behind a thin layer of Cr_2O_3. This process explains the reduced wastage at temperatures above 500° C. At even higher temperatures, the increase in wastage can be attributed to removal of the thin Cr_2O_3 layer along with the metallic substrate.

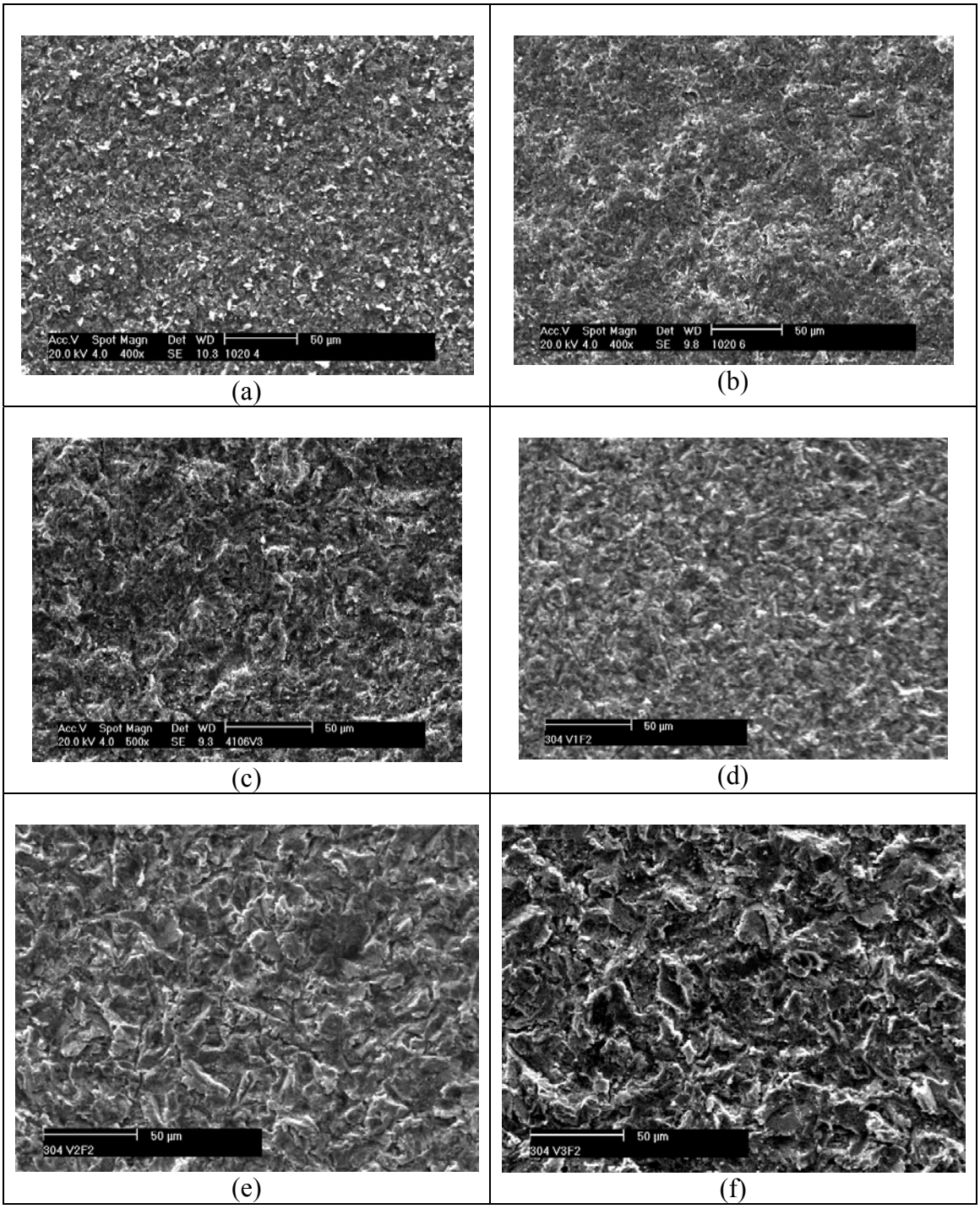

Figure 3. Scanning electron micrographs of the E-O tested steel surfaces. (a) AISI 1020, 5h at R.T.; (b) AISI 1020, 5h at 300° C; (c) AISI 410, 5h at 600° C, V3; (d) AISI 304, 5h 600° C at V1; (e) AISI 304, 5h 600° C at V2; (f) AISI 304, 5h 600° C at V3.

3.3 Surface Features of E-O Tested Steel Specimens

The surfaces of all the steel specimens E-O tested at the various temperatures for 5 h and at the different particle impact velocities were examined in a SEM and specific

regions analyzed. Some of the main features were: (a) embedded alumina particles on specimen surfaces (figure 3a). On specimens E-O tested at higher temperatures few embedded particles were observed. Similar observations were reported by Stack et. al.[12]; (b) erosion of the substrate. (Figure 3b); (c) the overall appearance of the E-O tested specimen surfaces were coherent with the wastage curves of the steels; (d) platelet formation on the surfaces of all the steels E-O tested at 600° C and at V3. (Figure 3c); (e) the effect of impact velocity on specimen surfaces was evident and revealed substrate removal and platelet formation. (Figure 3d-f)

3.4 Erosion-oxidation Mechanisms

In general terms, wastage increases with increase in temperature up to a certain maximum value (critical temperature) and then decreases with further increase in temperature. This value in the wastage versus temperature curve shifts to higher temperatures and to higher wastage with increase in erosive particle impact energy and increase in oxidation resistance of the alloy. The reasons put forth to explain this behavior are many and one that has been reasonably accepted is : at low temperatures the dominant process is erosion of the metal and wastage is ' erosion dominated'. With increase in temperature, oxide formation increases exponentially. If this oxide is significantly less resistant to erosion than the substrate, it is removed along with the substrate with increase in temperature at successive erosive events. Since oxidation rates increase markedly with temperature this indicates that at a specific temperature the wastage due to loss of oxide is higher than wastage due to loss of metal. This marks the wastage transition to 'erosion-oxidation-dominated'. If the oxide continues to be removed by particle impact, the wastage increases with increase in temperature (increase in oxidation rate). However, at a certain critical temperature, the oxide formed between successive particle impacts attains a thickness and cohesion that are sufficient not to be removed to the oxide-metal interface. This marks the transition to 'oxidation dominated'. Above this temperature the general loss of weight decreases with increase in temperature.

3.5 Erosion-oxidation Maps

Low, moderate and severe wastage values of the steels were specified: low as: > - 4,0 x 10^{-5} mg.mm^{-2}; moderate as > - 4,0 x 10^{-5} < -1,0 x 10^{-4} mg.mm^{-2} ; severe as : > -1,0 x 10^{-4} mg.mm^{-2} . These values were based on data from literature about acceptable levels of degradation of industrial components exposed to aggressive atmospheres. On the basis of these values, E-O wastage maps of the steels were prepared as a function of temperature and particle impact velocity. In these maps, shown in figure 4, the low, moderate and severe wastage zones have been indicated with white, light grey and dark grey areas.

As a general orientation, the white and light grey regions in these maps indicate the temperature and particle impact velocity conditions under which these steels can be used for various applications in a number of industries. More data is required to improve these maps. These include: (a) lower and higher particle impact velocities; (b) other temperatures; (c) particle impact angles.

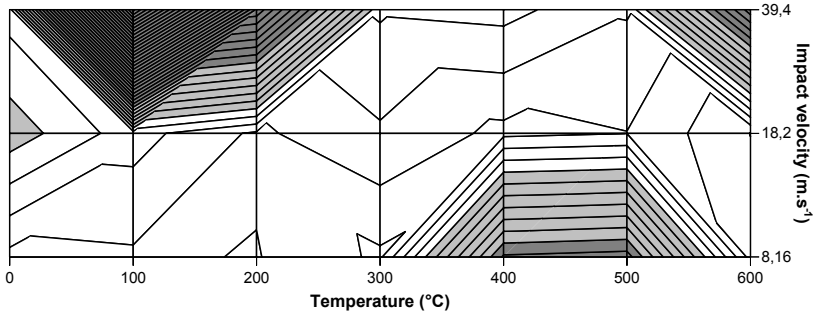

(a)

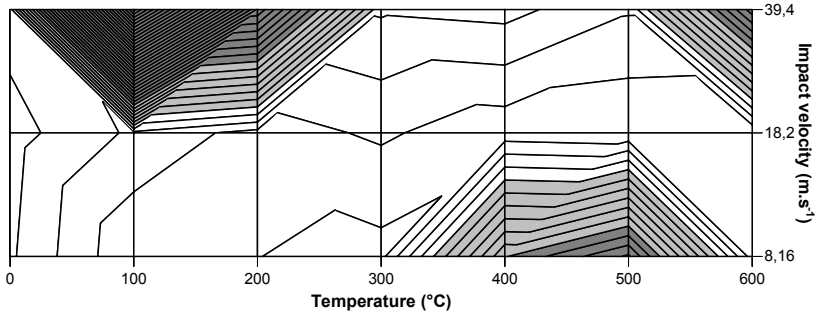

(b)

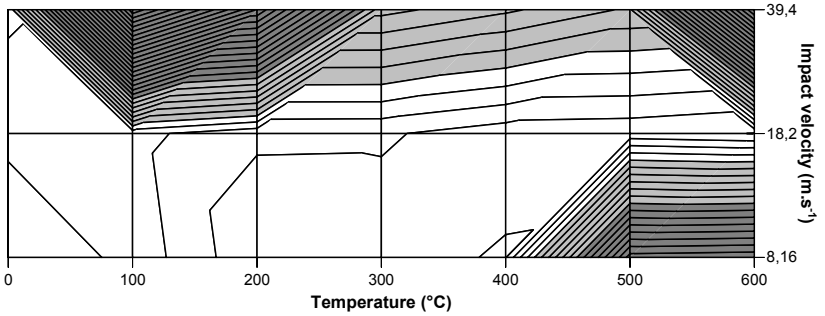

(c)

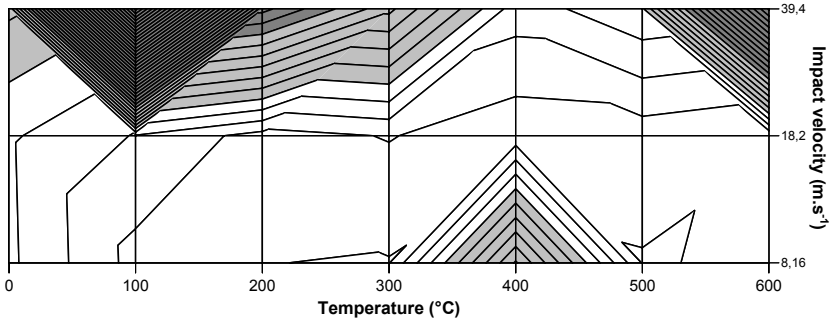

(d)

Figure 4. E-O wastage maps of the steels: (a) AISI 1020; (b) AISI 410; (c) AISI 304 ; (d) AISI 310.

4 CONCLUSIONS

1. The oxidation behavior of all the steels except AISI1020, were parabolic. The oxides formed on the steel surfaces were: (a) AISI 410 - Fe_2O_3 e $(Fe, Cr)_2O_3$; (b) AISI 304 - Fe_2O_3, Fe_3O_4, Cr_2O_3; (c) AISI 310 - Cr_2O_3.
2. The E-O transition temperatures of the steels as a function of PIV varied: (a) AISI 1020 shifted from 450° C at V1 to 500° C at V2 to > 600° C at V3; (b) AISI 410 shifted from 500° C at V1 to > 600° C at V3; (c) AISI 304 did not shift from 500° at V1 and V2 but shifted to > 600° C at V3; (d) AISI 310 shifted from 400° C to 510° C to > 600° C with increase in PIV from V1 to V2 to V3.
3. E-O maps were prepared as a function of PIV and temperature. Low, moderate and severe wastage zones were indicated in these maps to aid in materials selection for industrial application of these steels.

REFERENCES

1 SHEWMON, P.; SUNDERARAJAN, G. The erosion of metals, **Annual Review of Materials Science**, v. 13, p. 301, 1983.
2 BITTAR, J.G.A. A study of erosion phenomena, Part I. **Wear**, v. 6, p.5.1963.
3 HUTCHINGS, I.M.; WINTER, R.E. Particle erosion of ductile metals – mechanism of material removal, **Wear**, v. 27, p.121, 1974.
4 WELLMAN, R.G.; NICHOLLS, J.R. High temperature erosion-oxidation mechanisms, maps and models, **Wear**, v. 256, p.907. 2004.
5 KALIDAKIS, S; STOTT, F.H. Erosion-corrosion of alloys in power plant heat exchangers at elevated temperatures, **Materials Science Forum**, v. 461-464, p.1031. 2004.
6 NORLING, R.; OLEFJORD, I. Erosion-corrosion of iron and nickel based alloys at 550° C. **Wear**, v. 254, p.173, 2003.
7 STACK, M.M.; LEKATOS, S,; STOTT, F.H. Erosion-corrosion regimes: number, nomenclature and justification, **Tribology International**, v. 28, p.445,1995.
8 KANG, C.T.; PETTIT, F.S.; BIRKS, N. Mechanisms in the simultaneous erosion-oxidation attack of nickel and cobalt at high temperatures, **Metallurgical Transactions**, v. 18A, p.1785, 1987.
9 RISHEL, D.M.; PETTIT, F.S.; BIRKS, N. Some principle mechanisms in the simultaneous erosion and corrosion attack of metals at high temperatures, **Materials Science and Engineering A**, v. 143, p.197, 1991.
10 STEPHENSON, D.J.; NICHOLLS, J.R. Modeling erosive wear, **Corrosion Science**, v. 35, p.1015, 1993.
11 STACK, M.M.; STOTT, F.H.; WOOD, G.C. Review of mechanisms of erosion-corrosion of alloys at elevated temperatures, **Wear**, v. 162-164(B), p.706, 1993.
12 STACK, M.M.; CHACON-NAVA, J.G.; STOTT, F.H. Synergism between effects of velocity, temperature and alloy corrosion resistance in laboratory simulated fluidized bed environments, **Materials Science and Engineering**, v.11, p1180, 1995.